Fuel 410 (2026) 137934

Contents lists available at ScienceDirect

Fuel

journal homepage: www.elsevier.com/locate/fuel

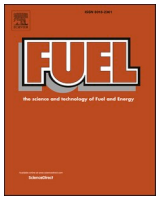

Full Length Article

5-hydroxymethylfurfural and furfural production in biphasic systems: kinetic studies of autocatalytic operation and using EDTA as thermoresponsive catalyst

Nico Thanheuser [a], Sebastian Püschel [a], Andreas J. Vorholt [a,*], Jesús Esteban [b,c,**]

[a] Max-Planck-Institute for Chemical Energy Conversion, Stiftstraße 34, 45470 Mülheim an der Ruhr, Germany
[b] Department of Chemical Engineering and Materials, Faculty of Chemical Sciences, Complutense University of Madrid, Madrid 28040, Spain
[c] Department of Chemical Engineering, School of Engineering, The University of Manchester, Manchester M13 9PL, United Kingdom

ARTICLE INFO

Keywords:
Furans
Biomass
Process intensification
Thermoresponsive catalyst
Kinetic studies
In situ product removal

ABSTRACT

5-hydroxymethylfurfural (HMF) and furfural are highly praised chemicals in the biofuel context, derived from fructose (Fruc) and xylose (Xyl), respectively. Here a H_2O/MIBK biphasic system is used as a green approach to extract *in situ* the furans generated in each reaction, thereby mitigating undesired reactions of rehydration and/or self-condensation to humins. The production of HMF and furfural is performed through two approaches: an autocatalytic reaction and using a thermoresponsive catalyst, hence facilitating recycling. Ethylenediaminetetraacetic acid (EDTA) was identified as a thermoresponsive organic acid with high recyclability (>97 % catalytic activity recovery after 5 cycles and regeneration) acting as homogeneous catalyst under reaction conditions. After proving the lack of mass transfer limitations and considering the reaction networks and mass balances for HMF and Fur production, macrokinetic models were proposed to describe the two reactions in a biphasic medium. In the autocatalytic regime, the values of the activation energy of the dehydration of Fruc to HMF and Xyl to furfural were 155.72 ± 12.84 kJ mol^{-1} and 138.09 ± 7.45 kJ mol^{-1}, respectively, whereas in the presence of EDTA as catalyst, the dehydration of Fruc to HMF showed a value of 139.12 ± 8.40 kJ mol^{-1} and that of Xyl to furfural of 130.33 ± 9.49 kJ mol^{-1}.

1. Introduction

Owing to the increasing concern about resource efficiency and the challenges associated with fossil-based feedstocks, the use of biobased substrates for a more sustainable production of fuels has developed significantly in the last years. In this context, the production of 5-hydroxymethylfurfural (HMF) and furfural from lignocellulosic sugars has attracted great attention. These two furans have been featured in the list of top value-added chemicals from biomass of the US Department of Energy because of their great relevance in synthesis [1]. From HMF, chemicals like 2,5-furandicarboxylic acid (FDCA), a monomer for bioplastics [2], or dimethylfuran, a biofuel additive [3] can be obtained from oxidation or hydrogenation, respectively. In the case of furfural, most of its use goes to the production of furfuryl alcohol, another biofuel additive of interest [4]. Lately, its relevance for the production of biobased jet-fuels is also being noted [5].

Sugar dehydration to produce these furans requires acidic media and most commonly occurs in H_2O. However, undesired side reactions occur, mainly the production of degradation products by self-condensation (humins) and, in the case of HMF, the additional rehydration to levulinic and formic acid (LA and FA, respectively) [6,7]. To mitigate these reactions, biphasic media are used for *in situ* product removal [6,8], which also represents an approach to process intensification [9]. For the production of HMF from glucose and fructose, previous studies reported the use of H_2O/2-MeTHF [10] and H_2O/MIBK media [11,12], a H_2O/$scCO_2$ [13] or H_2O/THF system where the aqueous phase is saturated with NaCl [14]. As for the synthesis of furfural from the dehydration of xylose, previous works studied the biphasic production using H_2O/DMC [15], H_2O/MIBK [16] or H_2O/high-pressure CO_2 [17]. Among the solvents tested, MIBK is the most

* Corresponding author.
** Corresponding author at: Department of Chemical Engineering and Materials, Faculty of Chemical Sciences, Complutense University of Madrid, Madrid 28040, Spain.
E-mail addresses: andreas-j.vorholt@cec.mpg.de (A.J. Vorholt), jeesteba@ucm.es, jesus.estebanserrano@manchester.ac.uk (J. Esteban).

https://doi.org/10.1016/j.fuel.2025.137934
Received 2 September 2025; Received in revised form 3 November 2025; Accepted 3 December 2025
Available online 12 December 2025

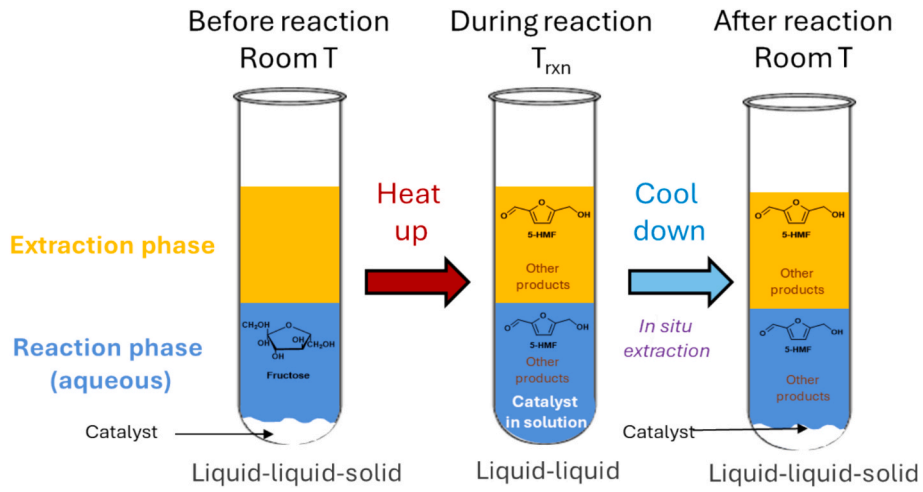

Fig. 1. Concept of the application of thermoresponsive catalysts in the biphasic production of HMF.

recurrently used extraction phase used owing to the high partition coefficients offered for both furans and its green credentials [6].

Reports on these reactions describe the use of a wide array of catalysts, including homogeneous like HCl [18], $FeCl_3$.6 H_2O [19] or $FeSO_4$ [20] and heterogeneous catalysts, such as ion exchange resins [21,22], zeolites [23,24] or heteropolyacids [25,26]. Homogeneous catalysts present the advantage of being soluble in the reaction phase acting as molecular catalysts, there not being mass transfer limitations by diffusional effects; on the other hand, their recyclability is limited. To circumvent the limitations to mass transfer in heterogeneous catalysts and enhance catalyst recyclability, there have been attempts at performing chemical reactions with materials showing thermoresponsive behaviour [27,28]. This poses an ingenious approach to multiphase reaction systems avoiding the inclusion of an additional phase during operation, as schematized in Fig. 1. Along these lines, Cao et al. showed the use of ethylenediaminetetraacetic acid (EDTA) as Brønsted acid catalyst to obtain HMF from fructose with excellent recyclability [29]. In addition, the production of HMF and Fur has also been tackled in the absence of catalyst by thermal or autocatalytic effect in monophasic media using conventional heating [30], in some cases under significant pressure (10 MPa) [31], highlighting the possibility of operating the without the need of thinking about catalyst recycling and possible diffusional effects.

For eventual reactor design, knowledge of the reaction kinetics is essential and despite the fact that there are studies on the kinetic modelling of the dehydration of sugars to furans in single liquid phase media [32–38], this type of studies is still scarce for LL systems [7]. Considering the relevance of these two furans in the future of biorefineries and the need to obtain kinetic information to explore further process development and reactor design, in this work we approach the production of HMF and furfural. The reactions are performed in biphasic media using MIBK as a benchmark green solvent [39] whilst avoiding the use of heterogeneous catalysts. First, the autocatalytic production of both furans is presented as the simplest biphasic system system for obtaining HMF and Fur. This was followed by the selection and use of a thermoresponsive organic acid to use as a proxy for a homogenous catalyst during the chemical reaction. For all cases, detailed macrokinetic models to describe the progress of the biphasic operation accounting for the phenomena involved are proposed.

2. Materials and methods

2.1. Materials

5-hydroxymethylfurfural (Fluorochem, 98 %), furfural (Sigma Aldrich, 99 %), fructose (ABCR, 99 %). levulinic acid (Sigma Aldrich, 98 %), formic acid (Merck, 98–100 %) were used for calibration. MIBK (Sigma Aldrich, >99 %), was used as extraction phase. EDTA (Sigma Aldrich, >99 %), phthalic acid ABCR, 99.5 %), isophthalic acid (Sigma Aldrich, 99 %), terephthalic acid (Sigma Aldrich, 98 %) and *o*-toluic acid (Sigma Aldrich, 99 %) were used for catalyst screening. MilliQ water filtered by Merck Millipak 0.22 μm (resistivity of 18.2 MΩ.cm) was used as reaction phase.

2.2. Selection of a thermoresponsive catalyst

A recoverability test is proposed for catalyst selection: 0.1 g L^{-1} of the organic acids tested were loaded in a batch of 4 mL of water and 12 mL of MIBK, heated up for dissolution to 150 °C as representative temperature of reaction for 10 min and then cooled down to room temperature for precipitation. These experiments were conducted in 30 mL glass vials with reinforced walls to withstand high pressures generated by the vapour pressure, which were heated up in an Anton Paar Monowave 450 microwave device. The catalyst was weighed after filtering the solid with a Buchner filter and evaporating the excess solvent overnight in an oven at 80 °C.

The thermal stability of the selected catalysts was evaluated by thermogravimetric analysis (TGA) making use of a TA Instruments Q500 device under N_2 with 50 ml/min flow from room temperature to 400 °C and a ramping rate of 10 °C /min.

2.3. Reaction procedure

In a typical experiment, 400 mg of fructose (2.22 mmol) or xylose (2.66 mmol), 4 mL of water and 12 mL of MIBK were loaded into 30 mL vials for operation in the microwave reactor. The catalytic experiments included, in addition, 40 mg of EDTA (1 % wt. with respect to the sugars). The reactions were run at temperatures between 140 and 170 °C and then cooled down in the Anton Paar Monowave 450 device before quenching quickly in an ice bath. These were run in constant temperature mode, with the power input fluctuating as a function of time to achieve the set temperature value. As a consequence of this, constant pressure values are generated by the evaporation of the solvents at these temperatures, which remain constant throughout the reaction, as measured by the non-invasive hydraulic pressure sensor system integrated in the cover of the Anton Paar Monowave 450 instrument. Samples were taken from the aqueous and organic phase with hypodermic needles to minimize disruption of the interphase.

For catalyst recycling, a procedure explained elsewhere was used, basically consisting of filtering the EDTA out of the reaction and

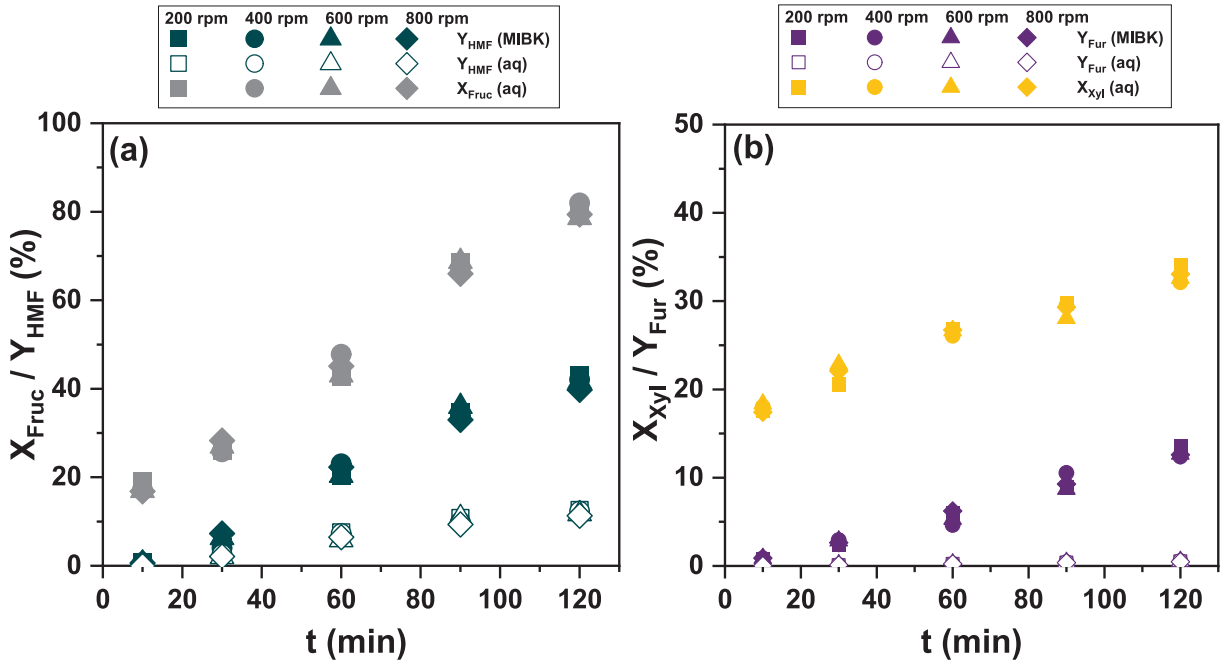

Fig. 2. Assessment of the effect of stirring on reaction performance for the production of (a) HMF and (b) furfural. Conditions: H_2O:MIBK = 1:3 v/v (V_{H2O} = 4 mL; V_{MIBK} = 12 mL); T = 150 °C; $C_{substrate}$ = 10 % wt·H_2O; C_{EDTA} = 1 wt% substrate. NOTE: Y_{HMF} (MIBK) and Y_{HMF} (aq) represent the yields to HMF as measured from the organic and aqueous phases, respectively; X_{Fruc} (aq) represents the conversion of Fruc as measured from the aqueous phase; Y_{Fur} (MIBK) and Y_{Fur} (aq) represent the yields to Fur as measured from the organic and aqueous phases, respectively and X_{Xyl} (aq) represents the conversion of Xyl as measured from the aqueous phase.

washing. For regeneration, the EDTA catalyst was dissolved in 5 mM of NaOH to eliminate the humins by filtration and EDTA was recrystallized with HCl 0.1 M [29]. The catalyst recycling tests were performed in triplicate.

Sample analysis for the aqueous phase was made with HPLC, whereas the organic extraction phase was analysed by a GC barrier discharge ionization detector (GC-BID), with details of the programs explained in our previous reference [40]. GC-BID enabled the detection of formic acid, as observed in Fig. S1, which is not possible with GC-FID.

2.4. Mathematical methods

Kinetic modelling for this work was performed on Aspen Custom Modeler V.12.1. The program applies a Levenberg-Marquardt algorithm integrating numerically via a fourth-order Runge-Kutta method. The fitting procedure started by correlation of a given model to the experimental data at a fixed temperature individually to obtain a first estimate of the activation energy. Then, the correlation was made with all the available observations at all temperatures incorporating the Arrhenius equation. The goodness of fit for the model is given by the residual mean squared error (RMSE) and the variation explained (VE), as detailed in section S2 of the Supplementary Information [41].

Finally, conventional magnitudes to evaluate catalytic performance, namely conversion, yield and selectivity, are defined in equations S6-S8 (Section S3). These consider the volume of each phase, which may undergo changes, as described by equations S10-S13, originally proposed elsewhere [11].

3. Results and discussion

3.1. Preliminary considerations for the simplification of the kinetic models

To evaluate the intrinsic reaction macrokinetics in multiphase systems, it is crucial to ensure that no mass transfer limitations occur. A preliminary experiment tested the stirring rate to assess its effect in the presence of a catalyst. As shown in Fig. 2, the performance difference is negligible at all rates, even 200 rpm. This agrees with previous works in biphasic systems [11,23,42]. To ensure that no phenomena other than chemical reaction is assessed, 400 rpm will be chosen subsequent analysis.

Another aspect to regard is the effect of temperature on heating, possible volume changes and catalyst dissolution rates, where applicable. The use of the microwave setup ensured reaching the set temperatures in about 60 s (Fig. S2), which is negligible compared to the overall length of the kinetic experiments; hence, it can be considered that the set temperature is reached instantaneously and the dependence with respect to this variable can be ignored. Additionally, when a thermoresponsive catalyst is used, the dissolution phenomenon can be considered to occur instantaneously (Fig. S3), which means that the acidity given by the dissociation of the catalyst, is fully available from the start of the reaction. Finally, despite the limited miscibility of H_2O and MIBK, there is a volume change that needs consideration in the concentration of each component. Equations S10 and S11 feature a correction factor representing this change. In a previous study, correlations were developed to account for the effect of temperature on this correction to the volume of each phase. These are summarised in equations S12 and S13, with the values of the correction factors featured in Table S1 [11].

3.2. Description of the kinetic models

3.2.1. Reaction pathway and modelling the production of HMF (reaction a)

Different kinetic models have been proposed for the dehydration of sugars to HMF (henceforth denoted as reaction *a*), as summarised in a previous review [7]. Based on the most common models reported in literature starting from fructose (Fruc), this compound is dehydrated to HMF (reaction $r_{1,a}$). Simultaneously, Fruc has been reported to degrade in two different ways by self-condensation, one leading to humins ($r_{4,a}$) and generating both humins and formic acid as by-product ($r_{3,a}$). In addition, even though the biphasic system tries to mitigate their progress, HMF can also degrade to humins ($r_{5,a}$) as well as undergo rehydration to LA and FA ($r_{2,a}$). Beyond the chemical reactions in the

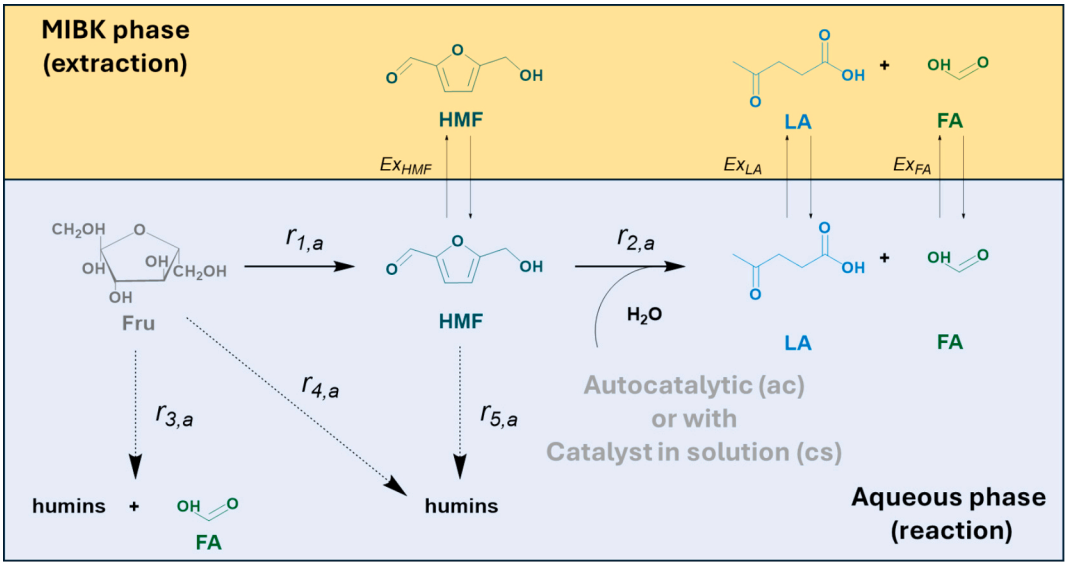

Fig. 3. Reaction network proposed for the biphasic production of HMF from Fruc and by-products with *in situ* extraction. Note that this reaction is denoted as *a* and the cases for the autocatalytic reaction will be *ac* and with catalyst in solution will be *cs*.

network, one must consider the extraction of HMF, LA and FA to the MIBK phase (symbolised by Ex_{HMF}, Ex_{LA} *and* Ex_{FA}, respectively), which occur to different extents considering the different partitioning of HMF, LA and FA. The extraction of Fruc to the organic phase has been neglected completely. These reactions and *in situ* extractions are schematized in Fig. 3.

As discussed in our review [7], there is a consensus that the aforementioned reactions are elementary and, therefore, can be expressed by Eqs. (1-5):

$$r_{1,a} = k_{1,a} C_{H^+} C_{Fruc,aq} \tag{1}$$

$$r_{2,a} = k_{2,a} C_{H^+} C_{HMF,aq} \tag{2}$$

$$r_{3,a} = k_{3,a} C_{H^+} C_{Fruc,aq} \tag{3}$$

$$r_{4,a} = k_{4,a} C_{H^+} C_{Fruc,aq} \tag{4}$$

$$r_{5,a} = k_{5,a} C_{H^+} C_{HMF,aq} \tag{5}$$

Here the k_i terms represent the kinetic constants, with a temperature dependence governed by the Arrhenius equation. In linear form, this is described by Eq. (6):

$$lnk_i = lnk_{i,0} - \frac{E_{a,i}}{R}\frac{1}{T} \tag{6}$$

where $k_{i,0}$ is the pre-exponential factor, $E_{a,i}$ is the activation energy of reaction *i* and *R* is the ideal gas constant. In Eqs. (1-5), the subscript *aq* refers to the reaction proceeding in the aqueous phase. In addition, it is worthwhile noting two aspects. First, the rehydration reaction represented by $r_{2,a}$ takes place in a large excess of water owing to it being the medium and thus becomes part of what could be considered and apparent constant $k_{2,a}$. In addition, as is well known, these reactions require the presence of an acidic medium to proceed. As the reaction progresses, the Brønsted acidity of the aqueous medium, in which it proceeds, will change owing to the increasing presence of the by-products contribution [13]. The protons present in the medium can be described by Eq. (7):

$$C_{H+} = C_{H+,EDTA} + C_{H+,H2O} + C_{H+,LA} + C_{H+,FA} + C_{H+,Fruc} + C_{H+,HMF} \tag{7}$$

This equation can be simplified. First, the protons generated by Fruc and HMF can be considered negligible owing to their very low dissociation constants (see pK_a values in Table S2). The concentration of protons generated by EDTA, LA, FA and H_2O can be seen in equations S14, S15, S16 and S17, respectively, as a function of the dissociation constants shown in Table S2. In the case of the autocatalyzed reaction, the protons generated by EDTA do not apply.

Considering the reaction pathway shown in Fig. 3, the mass balances for each component are:

$$\frac{dC_{Fru,aq}}{dt} = -r_{1,a} - r_{3,a} - r_{4,a} \tag{8}$$

$$\frac{dC_{HMF,aq}}{dt} = r_{1,a} - r_{2,a} - r_{5,a} - Ex_{HMF} \tag{9}$$

$$\frac{dC_{HMF,MIBK}}{dt} = Ex_{HMF} \tag{10}$$

$$\frac{dC_{LA,aq}}{dt} = r_{2,a} - Ex_{LA} \tag{11}$$

$$\frac{dC_{LA,MIBK}}{dt} = Ex_{LA} \tag{12}$$

$$\frac{dC_{FA,aq}}{dt} = r_{2,a} + r_{3,a} - Ex_{FA} \tag{13}$$

$$\frac{dC_{FA,MIBK}}{dt} = Ex_{FA} \tag{14}$$

In the previous set of equations, it is noteworthy to mention that no extraction of Fru has been considered (Eq. (8)) owing to its lack of solubility in MIBK, contrary to the rest of the components involved in the reaction scheme (Eqs. (9-14)). As demonstrated in Section 3.1, no mass transfer limitations are present and hence the extraction of each of HMF, LA and FA can be considered instantaneous. The partition coefficient of each compound *j* (PC_j) in the aqueous and the MIBK phases acts as proportionality factors between their concentrations and can be defined as:

$$PC_j = \frac{C_{j,MIBK}}{C_{j,aq}} \tag{15}$$

Neglecting the extraction rates of each of the compounds owing to the lack of mass transfer limitations explained in Section 3.1, Eqs. (9-14) can be rewritten considering the *PC* as a ratio between the concentrations in

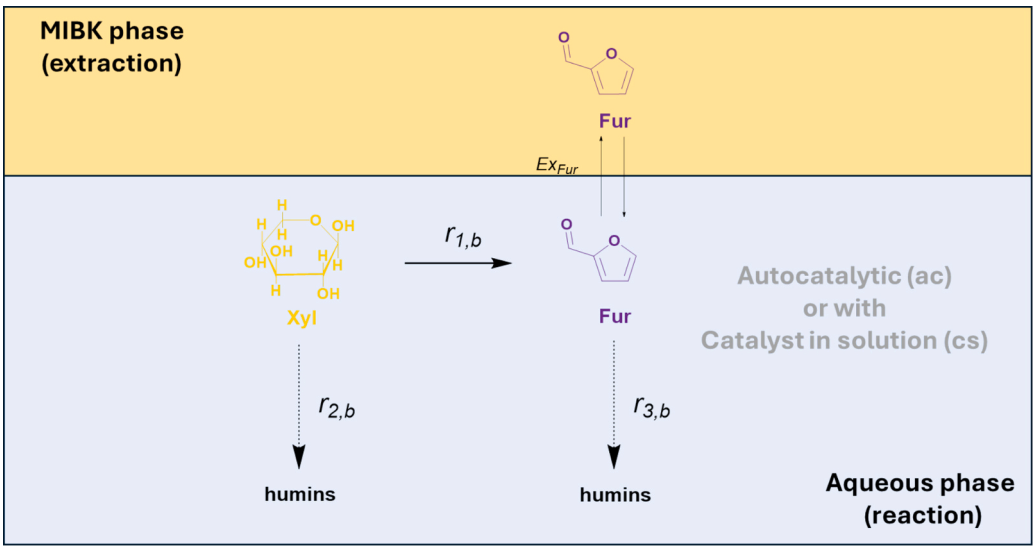

Fig. 4. Reaction network proposed for the biphasic production of Fur with its *in situ* extraction starting from Xyl. Note that this reaction is denoted as *b* and the cases for the autocatalytic reaction will be *ac* and with catalyst in solution will be *cs*.

the organic and the aqueous phase, through Eqs. (16-21). This approach has been used previously [11,16,42].

$$\frac{dC_{HMF,aq}}{dt} = \frac{r_{1,a} - r_{2,a} - r_{5,a}}{1 + PC_{HMF}} \tag{16}$$

$$\frac{dC_{HMF,MIBK}}{dt} = PC_{HMF} \bullet \frac{dC_{HMF,aq}}{dt} \tag{17}$$

$$\frac{dC_{LA,aq}}{dt} = \frac{r_{2,a}}{1 + PC_{LA}} \tag{18}$$

$$\frac{dC_{LA,MIBK}}{dt} = PC_{LA} \bullet \frac{dC_{LA,aq}}{dt} \tag{19}$$

$$\frac{dC_{FA,aq}}{dt} = \frac{r_{2,a} + r_{3,a}}{1 + PC_{FA}} \tag{20}$$

$$\frac{dC_{LA,MIBK}}{dt} = PC_{FA} \bullet \frac{dC_{FA,aq}}{dt} \tag{21}$$

The *PC* values for HMF, LA and FA were estimated from the measurements taken in the kinetic experiments. For each experiment at a different temperature, an average was taken for each of the partition coefficients measured at a different reaction time to account for the possible influence may that the presence of other compounds may have globally. Fig. S4 represents all these values. Within the range of temperatures tested of 140 to 170 °C, it was found that there is a linear relationship between *PC* and temperature for HMF, whereas in the case of LA and FA, a practically constant value was obtained, as shown in equations S18-S20.

Finally, humins are calculated from the non-closure of the carbon balance (equation S9). Considering the reaction network, they can be generated from Fruc and HMF with a balance following:

$$\frac{dC_{Humins}}{dt} = r_{3,a} + r_{4,a} + r_{5,a} \tag{22}$$

3.2.2. Reaction pathway and model for the production of furfural (reaction b)

Following a similar approach, a model is also proposed to describe the progress of the dehydration of xylose (Xyl) to Fur, denoted as reaction *b*. Here the reaction network only features the dehydration of Xyl to Fur ($r_{1,b}$) and the degradation to humins starting from either Xyl ($r_{2,b}$) or Fur ($r_{3,b}$). Also, the *in situ* extraction of Fur is considered (Ex_{Fur}). Fig. 4 shows these steps.

As in reaction *a*, the rates are considered to follow power-law models of first order with respect to each of the reactants both for the autocatalytic (*ac*) or with catalyst in solution (*cs*) cases:

$$r_{1,b} = k_{1,b} C_{H^+} C_{Xyl,aq} \tag{23}$$

$$r_{2,b} = k_{2,b} C_{H^+} C_{Xyl,aq} \tag{24}$$

$$r_{3,b} = k_{3,b} C_{H^+} C_{Fur,aq} \tag{25}$$

In this case, the acidity will correspond to protons generated from water and in the *ac* case and those by water and the EDTA catalyst in the *sc* case. Therefore, Eq. (7) should consider only their contribution.

From the reaction pathway in Fig. 4, the mass balances would be:

$$\frac{dC_{Xyl,aq}}{dt} = -r_{1,b} - r_{2,b} \tag{26}$$

$$\frac{dC_{Fur,aq}}{dt} = r_{1,b} - r_{3,b} - Ex_{Fur} \tag{27}$$

$$\frac{dC_{Fur,MIBK}}{dt} = Ex_{Fur} \tag{28}$$

Owing to Xyl not dissolving in MIBK, the mass balance in Eq. (26) does not contemplate its extraction into the organic phase. As shown in Fig. 2b, in the case of reaction *b*, no mass transfer limitations were observed, so the extraction of Fur can be assumed to take place immediately with its concentration in the MIBK phase being proportional to that of the aqueous phase being represented by the *PC* of Fur following Eq. (15). Therefore, the mass balances for Fur in the aqueous and MIBK phases can be expressed by:

$$\frac{dC_{Fur,aq}}{dt} = \frac{r_{1,b} - r_{3,b}}{1 + PC_{Fur}} \tag{29}$$

$$\frac{dC_{Fur,MIBK}}{dt} = PC_{Fur} \bullet \frac{dC_{Fur,aq}}{dt} \tag{30}$$

The value of PC_{Fur} was obtained from the concentrations analysed in each of the dynamic experiments at different temperatures. Fig. S4 shows that the value of PC_{Fur} changed between 7.45 at 140 C and 6.68 at 170 C, which is in close agreement by that shown by Huber et al. (approximately 7.1 in the same temperature range) [16] and Huang

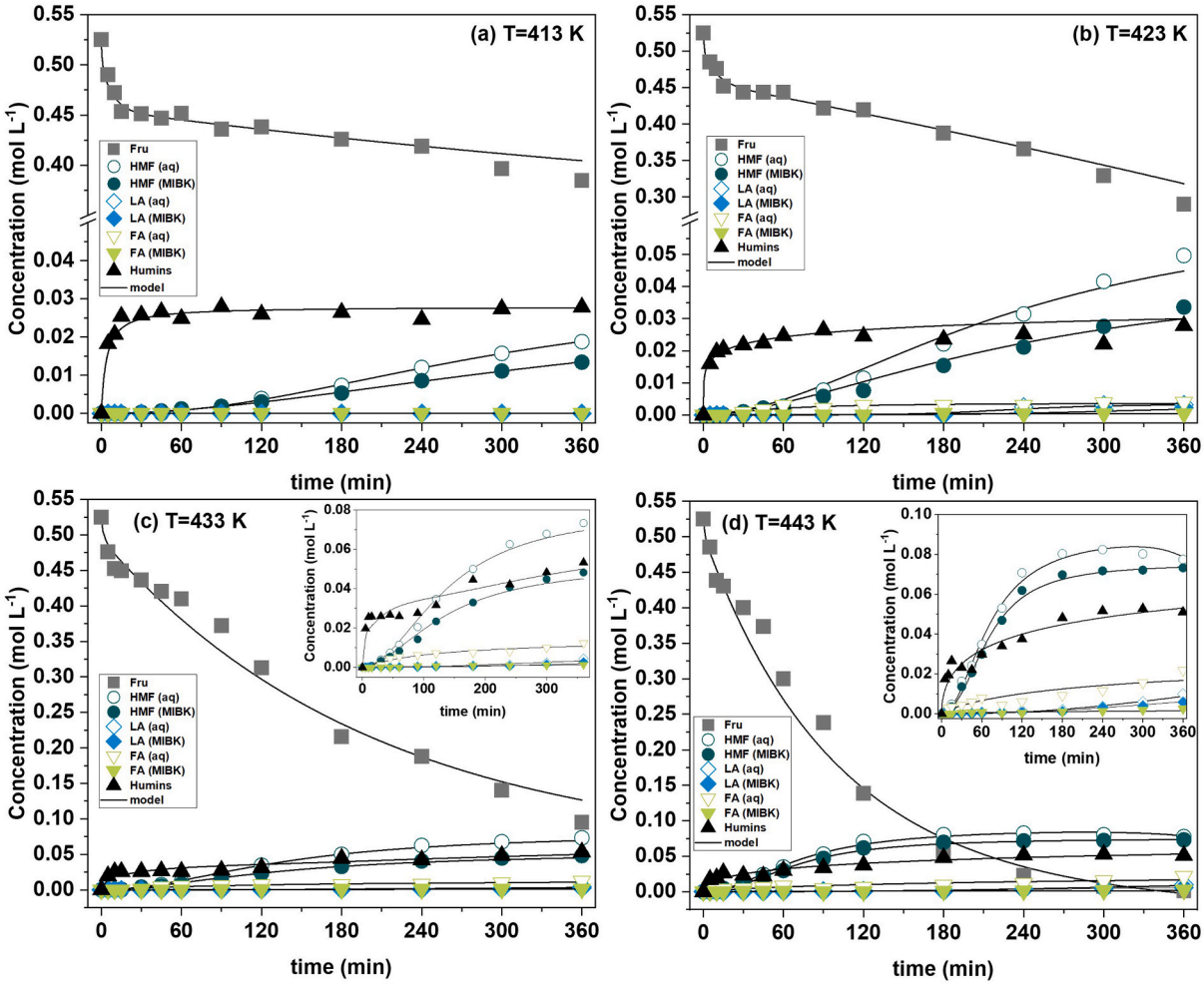

Fig. 5. Reaction profiles and fittings for the autocatalytic (*ac*) production of HMF (reaction *a*) at (a) T = 140 °C; (b) T = 150 °C; (c) T = 160 °C; (d) T = 170 °C. Conditions: H_2O/MIBK = 1:3 v/v (V_{H2O} = 4 mL; V_{MIBK} = 12 mL); $C_{substrate}$ = 10 % wt·H_2O; ω = 400 rpm.

Table 1
Kinetic parameters and goodness of fit obtained from the fitting of the model for the autocatalytic (*ac*) dehydration of Fruc to HMF (reaction *a*). Error in the parameters is given at 95% confidence interval.

Reaction	ln $k_{i,0}$ ± error	$E^{ac}_{a,i}/R$ ± error (K)	RMSE	VE (%)
$r^{ac}_{1,a}$	26.37 ± 3.95	18729 ± 1545	0.1278	96.41
$r^{ac}_{2,a}$	20.75 ± 3.81	12994 ± 1097		
$r^{ac}_{3,a}$	18.52 ± 3.01	17989 ± 1698		
$r^{ac}_{4,a}$	21.15 ± 3.08	14091 ± 1384		
$r^{ac}_{5,a}$	21.85 ± 2.49	8883 ± 747		

et al. (7.62 at 130 C) [43]. A linear variation was considered in our case following equation S21.

In this system, humins are also computed from the closure of mass balances through equation S9, where the evolution of their production can be described by equation (29) considering that they are assumed to be generated by reactions $r_{2,b}$ and $r_{3,b}$:

$$\frac{dC_{Humins}}{dt} = r_{2,b} + r_{3,b} \tag{31}$$

3.3. Autocatalytic reactions (ac)

H_2O by itself has proven to provide a viable medium to produce furans in the absence of additional catalysts in both reactions, thereby leading to autocatalytic reactions [30,44]. Fig. 5 shows the evolution of the concentration of the detectable species in each phase and the calculated humins for the autocatalytic reaction *a* in H_2O/MIBK between 140 and 170 °C. There is an obvious effect of temperature on reaction progress, where after 6 h, applying equations S6-S8, the conversion reached at 140 °C is only of X_{Fruc} = 30.1 %, at 150 °C of 46.4 %, at 160 °C of 82.7 % and only at 170 °C practically full conversion of the substrate was observed. The overall yields to HMF observed ranged from Y_{HMF} = 12.6 % at 140 C to 65.8 % at 170 °C, leading to selectivities of S_{HMF} = 41.9 % and 66 %, respectively. In the case of the reaction at 170 °C, the inset shows that the maximum concentrations of HMF are obtained at 4 h, which would lead to Y_{HMF} = 67.6 % and a remarkable S_{HMF} = 70.1 %. This maximum indicates that after this point, the degradation of HMF to obtain the by-products starts prevailing. In addition, the evolution of the soluble by-products LA and FA is worthwhile remarking. In particular, the experiments performed at 160 and 170 °C depict somewhat greater concentrations of FA, visible in the insets of Figs. 5c and 5d. This reinforces the hypothesis that not only is it generated by the rehydration of HMF (reaction $r_{2,a}$), but also from the degradation of Fruc ($r_{3,a}$), as also considered in other works [11,45]. Finally, the production of humins as an end by-product in the reaction network undergoes a steady increase. The facts that concentration maxima of HMF can be obtained together with humins, FA and LA continuously increasing, lead to think that selecting an appropriate operation time is key to increase the atom and carbon economy of the reaction and facilitate subsequent downstream separation processes. In

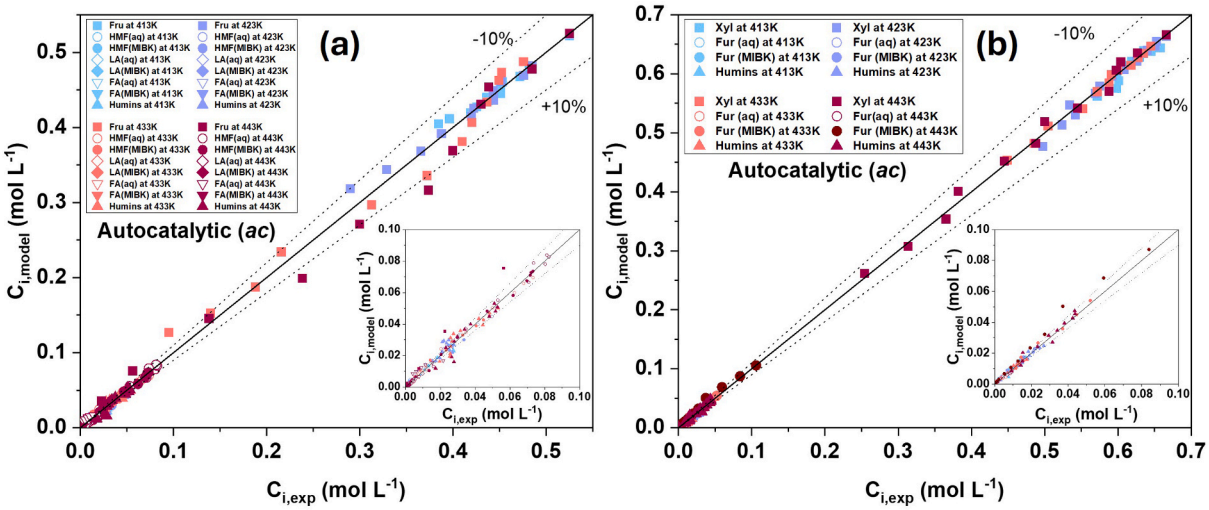

Fig. 6. Parity plots of the kinetic models proposed for the autocatalytic (*ac*) production of (*a*) HMF from Fruc and (*b*) Fur from Xyl.

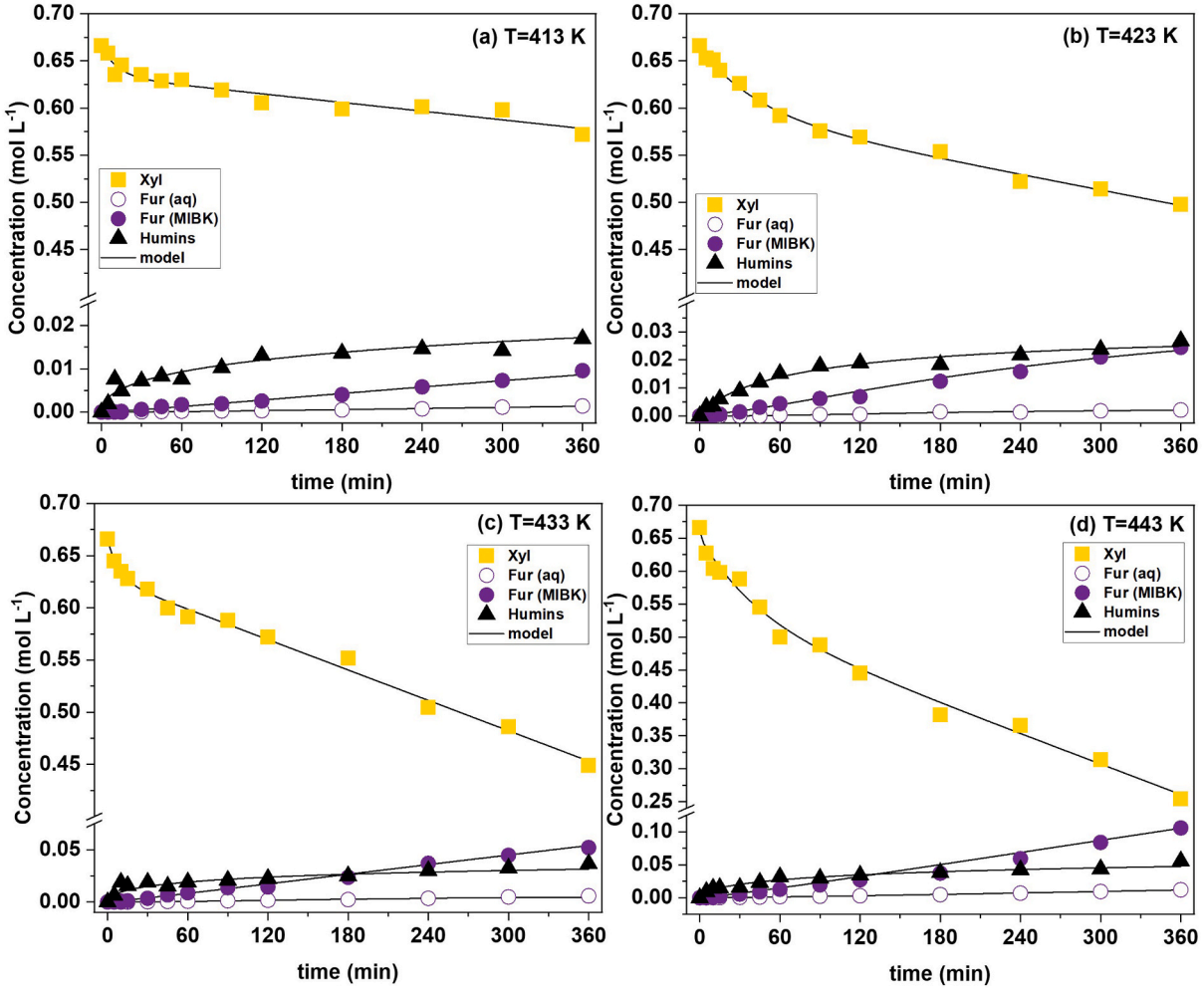

Fig. 7. Reaction profiles and fittings for the autocatalytic (*ac*) production of Fur (reaction *b*) at (a) T = 140C; (b) T = 150C; (c) T = 160C; (d) T = 170C. Conditions: H_2O/MIBK = 1:3 v/v (V_{H2O} = 4 mL; V_{MIBK} = 12 mL); $C_{substrate}$ = 10 % wt·H_2O; substrate; ω = 400 rpm.

this sense, operation in the absence of a catalyst could facilitate subsequent handling, although at the expense of lower reaction rates.

Jointly with the observed evolution of the species in the autocatalyzed reaction *a*, Fig. 5 also shows the values predicted by the model, which show a good fitting. The parameters are featured in Table 1, where the activation energies for the reactions translate into $E^{ac}_{a,1,a} = 155.72 \pm 12.84$ kJ mol^{-1}, $E^{ac}_{a,2,a} = 108.04 \pm 9.12$ kJ mol^{-1}, $E^{ac}_{a,3,a} = 149.56 \pm 14.11$ kJ mol^{-1}, $E^{ac}_{a,4,a} = 117.15 \pm 11.51$ kJ mol^{-1} and $E^{ac}_{a,5,a} =$

Table 2
Kinetic parameters and goodness of fit obtained from the fitting of the model for the autocatalytic (*ac*) dehydration of Xyl to Fur (reaction *b*). Error in the parameters is given at 95% confidence interval.

Reaction	ln $k_{i,0}$ ± error	$E_{a,i}^{ac}/R$ ± error (K)	RMSE	VE (%)
$r_{1,b}^{ac}$	25.08 ± 4.01	16609 ± 896	0.0953	97.16
$r_{2,b}^{ac}$	29.94 ± 4.38	16484 ± 1002		
$r_{3,b}^{ac}$	21.95 ± 3.18	8654 ± 765		

73.85 ± 6.21 kJ mol^{-1}. In addition, values of RMSE and VE as metrics for the goodness of fit, obtaining an error of 0.1155 and a variation explained ~97 %, both of which represent a high correlation. The ability of the model to describe the evolution of the species is also highlighted in Fig. 6a, which displays the parity plot for the autocatalytic reaction *a*. It may be seen that most results predicted by the model fall within a ±10 % error with respect to the parity line, except for the concentration of Fruc in the experiment conducted at 443 K, whose determination in this case suffered a higher experimental error.

The evolution of the experimental values and the model for the autocatalyzed reaction *b* between 140 °C and 170 °C is depicted in Fig. 7. Here the progress of the reaction is significantly lower in terms of conversion of the substrate than in the case of reaction *a*, with conversions of xylose ranging betweenX_{Xyl} = 13.3 %, at 140 °C andX_{Xyl} = 61.5 % at 170 °C after 6 h. In this case, the maximum yield and selectivity obtained within the tested time range were at 170C, whenY_{Fur} = 39.7 % andS_{Fur} = 64.5 %. The calculated production of humins sees an increase in all cases, yet the escalation does not appear to be too high with temperature. Table 2 compiles the parameters obtained from the correlation of the model, where the dehydration of Xyl to Fur ($r_{1,b}^{ac}$) had an activation energy of $E_{a,1,b}^{ac}$ = 138.09 ± 7.45 kJ mol^{-1}, the degradation of Xyl to humins ($r_{2,b}^{ac}$) of $E_{a,2,b}^{ac}$ = 137.05 ± 8.33 kJ mol^{-1}, and Fur to humins ($r_{3,b}^{ac}$) of $E_{a,3,b}^{ac}$ = 71.95 ± 6.36 kJ mol^{-1}. Fig. 7b presents the parity plot for the autocatalyzed reaction *b*, where there is a high agreement between the predicted and observed values. This goodness of fit is illustrated by an explained variation of 98.54 % and a RMSE of 0.0804.

Likozar et al. studied the kinetics of both reactions *a* and *b* in the absence of catalyst, which was the only study found of these characteristics [30]. For *a*, the reaction network was somewhat different to this work since the conversion of glucose as a substrate was contemplated, which entails an isomerisation step in equilibrium with Fruc. On the other hand, they did not report the generation of LA from the rehydration of HMF or FA by this reaction or the direct production from Fruc. Additionally, their system is monophasic, meaning that there is no consideration of the extraction of any of the components involved into a second liquid phase. In terms of Fig. 3, the values reported for the activation energies of comparable reactions to this work were $E_{a,1,a}^{ac}$ = 139$kJmol^{-1}$, $E_{a,4,a}^{ac}$ = 120$kJmol^{-1}$ and $E_{a,5,a}^{ac}$ = 106$kJmol^{-1}$. In the case of reaction *b*, the reaction network was the same as in this study for which, again translating into the notation used in this work (Fig. 4), from their fittings they obtained $E_{a,1,b}^{ac}$ = 122$kJmol^{-1}$, $E_{a,2,b}^{ac}$ = 213$kJmol^{-1}$ and $E_{a,3,b}^{ac}$ = 71$kJmol^{-1}$. All of these values are comparable to the ones reported in Tables 1 and 2. However, contrary to our study in biphasic systems where temperature is reached almost instantaneously, they used monophasic aqueous systems where the heating was supplied by convection at a heating rate of 5 °C min^{-1} [30]. In their study, the consideration of the start time for their dehydration reactions took place once the set temperature was reached, which inevitably means that the reaction was already taking place for some time. These variations in the experimental approach may explain the differences in reaction performance and kinetic parameters.

3.4. Operation with catalyst in solution (cs)

3.4.1. Selection of a thermoresponsive catalyst and recyclability tests in reaction

Thermoresponsive systems can be defined as those that show multiphase behaviour at one temperature and a single phase at a different temperature, where the former temperature is typically lower than the latter [46]. Operating with a thermoresponsive catalyst allows performing reactions *a* and *b* at relevant temperatures in a biphasic regime (the MIBK phase is still needed to perform the *in-situ* extraction) without incorporating a solid phase whilst being able to recycle the catalyst after cooling. Table S3 compiles a survey of organic acids showing a change in their solubility in H_2O greater than an order of magnitude between room temperature and higher temperatures [47–50], which could be regarded as thermoresponsive. The reported values are at atmospheric pressure and therefore they cannot reach the reaction temperatures used in this work (140 – 170 °C), where autogenous pressure is reached from the vapour pressure of the solvents used.

To screen for a potential organic acid to act as catalyst, a recoverability test was conducted. For this, different organic acids were loaded

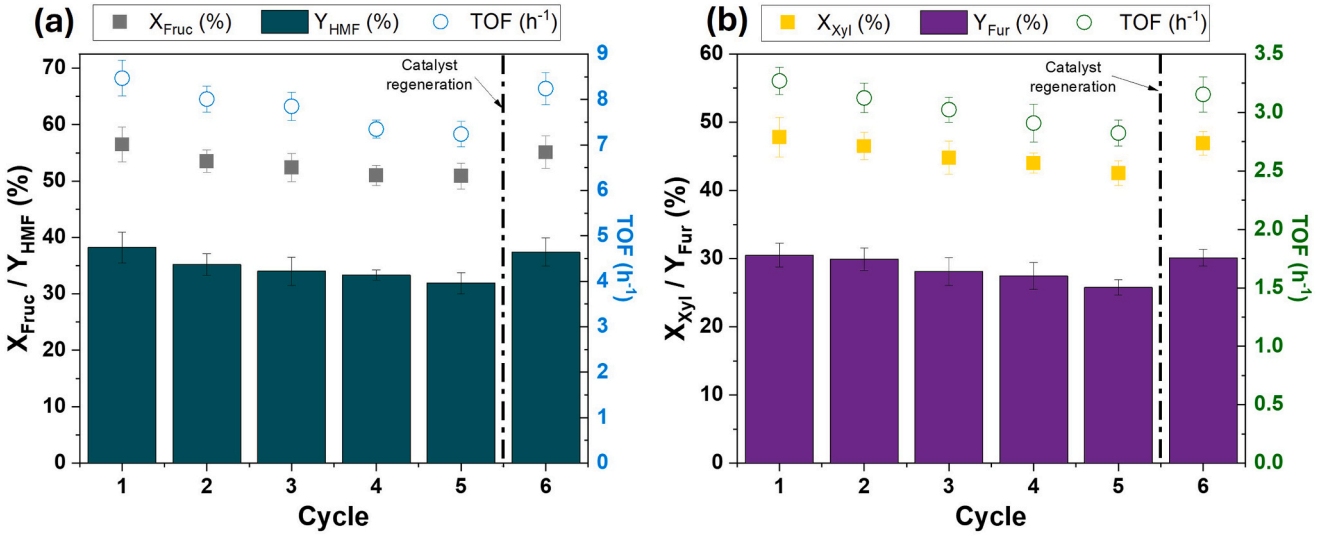

Fig. 8. Recyclability tests of EDTA in the production of (a) HMF at T = 423 K and t = 90 min and (b) Fur at T = 433 K and t = 240 min. Rest of common conditions: (a) T = 423 K·H_2O/MIBK = 1:3 v/v (V_{H2O} = 4 mL; V_{MIBK} = 12 mL); C_{solute} = 0.1 g L^{-1} H_2O; substrate; ω = 400 rpm.

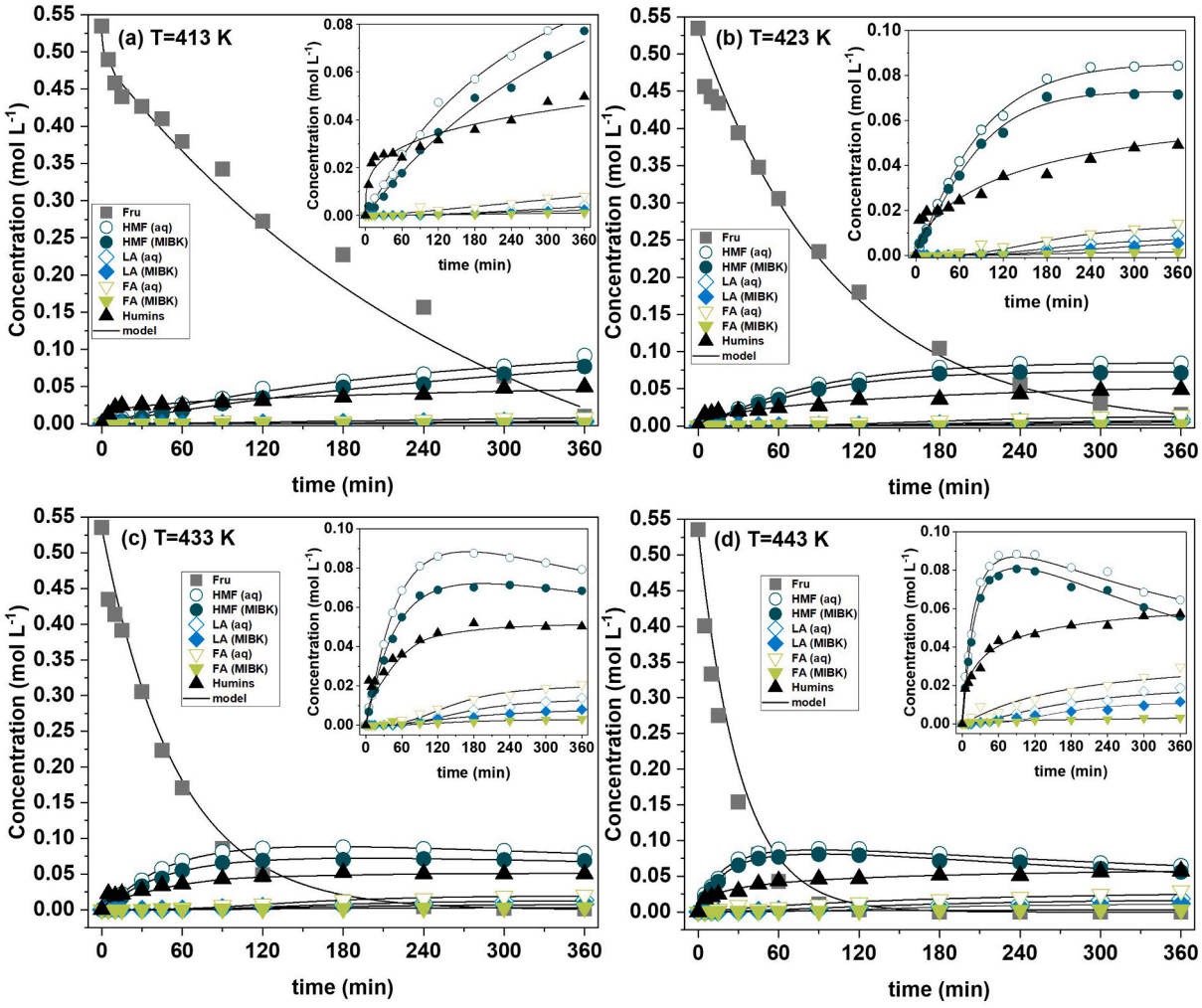

Fig. 9. Reaction profiles and model fittings for the production of HMF from fructose (reaction *a*) with EDTA as catalyst in solution (*cs*) at (a) T = 140C; (b) T = 150C; (c) T = 160C; (d) T = 170C. Conditions: H_2O/MIBK = 1:3 v/v (V_{H2O} = 4 mL; V_{MIBK} = 12 mL); $C_{substrate}$ = 10 % wt·H_2O; C_{EDTA} = 1 wt% substrate; ω = 400 rpm.

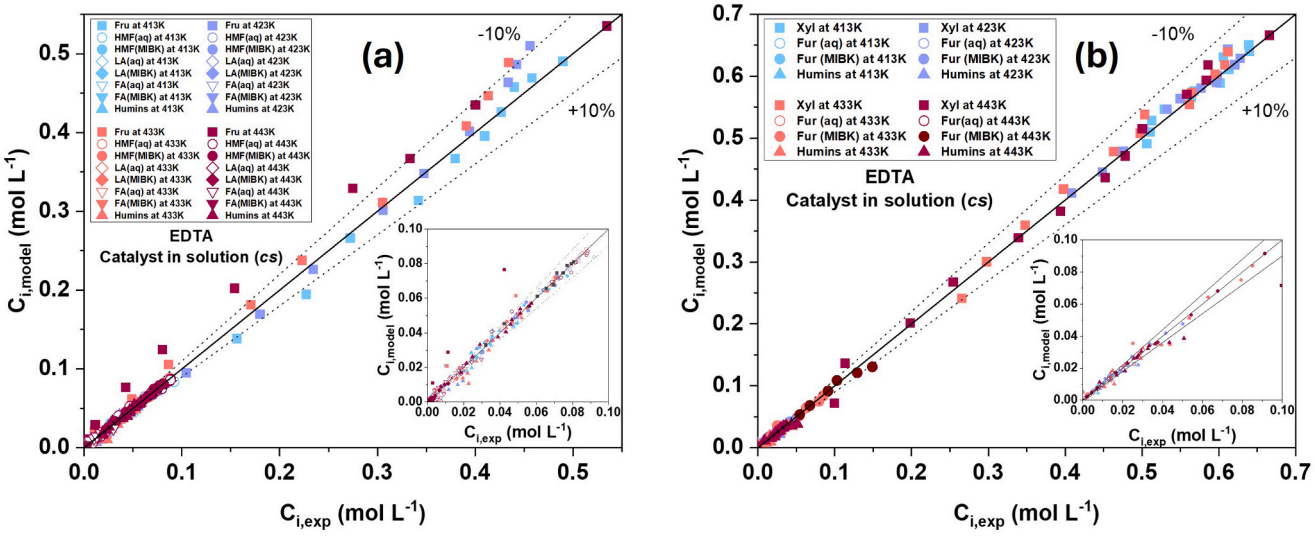

Fig. 10. Parity plots comparing the predicted and observed concentration profiles for the production of (*a*) HMF from Fruc and (*b*) Fur from Xyl with EDTA as catalyst in solution (*cs*).

Table 3
Kinetic parameters and goodness of fit obtained from the fitting of the model for the dehydration of Fruc to HMF (reaction *a*) with EDTA as catalyst in solution (*cs*). Error in the parameters is given at 95% confidence interval.

Reaction	ln $k_{i,0}$ ± error	$E^{cs}_{a,i}/R$ ± error (K)	RMSE	VE (%)
$r^{cs}_{1,a}$	31.11 ± 3.84	16733 ± 1010	0.1155	97.04
$r^{cs}_{2,a}$	23.57 ± 4.01	12337 ± 965		
$r^{cs}_{3,a}$	21.27 ± 5.66	16216 ± 1221		
$r^{cs}_{4,a}$	20.58 ± 5.46	11661 ± 884		
$r^{cs}_{5,a}$	19.76 ± 3.89	11733 ± 1051		

Table 4
Comparison of the activation energies of the reactions involved in the production of the dehydration of Fruc to HMF (reaction *a*) catalysed with EDTA in solution (*cs*) obtained in this work with others in literature starting from Fruc as substrate.

Reaction	Solvent system (aq:org v/v)	Catalyst	E_a(kJ mol^{-1})	T (K)	Ref.
$r^{cs}_{1,a}$	H_2O (monophasic)	LiCl·3H_2O 0.25 M	139.2	413–443	[55]
	H_2O (monophasic)	HCl 1 M	126 ± 2	343–423	[56,57]
	DMSO (monophasic)	MIL-101 (Cr)-SO_3H	55	373–413	[54]
	H_2O / GVL(1:9)	Triflic acid 10 mM	109 ± 4	353–393	[53]
	H_2O / MIBK (1:4) [a]	H_2SO_4 0.45 M	133 ± 5	393–433	[11]
	H_2O / MIBK (1:3)	EDTA	139.12 ± 8.40	413–453	This work
$r^{cs}_{2,a}$	H_2O (monophasic)	LiCl·3H_2O 0.25 M	72.7	413–443	[55]
	H_2O (monophasic)	HCl 1 M	97 ± 1	343–423	[56,57]
	H_2O / MIBK (1:4) [a]	H_2SO_4 0.45 M	97 ± 3	393–433	[11]
	H_2O / MIBK (1:3)	EDTA	102.57 ± 8.02	413–453	This work
$r^{cs}_{3,a}$	H_2O / MIBK (1:4) [a]	H_2SO_4 0.45 M	147 ± 20	393–433	[11]
	H_2O (NaCl)/THF (1:3) (6 mM NaCl)	$AlCl_3$ 2.5 mM	74	403–433	[45]
	H_2O / MIBK (1:3)	EDTA	134.82 ± 10.15	413–453	This work
$r^{cs}_{4,a}$	H_2O (monophasic)	LiCl·3H_2O 0.25 M	49.5	413–443	[55]
	H_2O (monophasic)	HCl 1 M	135 ± 8	343–423	[56,57]
	H_2O / MIBK (1:4) [a]	H_2SO_4 0.45 M	142 ± 13	393–433	[11]
	H_2O / MIBK (1:3)	EDTA	96.95 ± 7.35	413–453	This work
$r^{cs}_{5,a}$	H_2O (monophasic)	LiCl·3H_2O 0.25 M	54.4	413–443	[55]
	H_2O (monophasic)	HCl 1 M	62 ± 9	343–423	[56,57]
	H_2O / MIBK (1:4) [a]	H_2SO_4 0.45 M	108 ± 11	393–433	[11]
	H_2O / MIBK (1:3)	EDTA	97.55 ± 8.74	413–453	This work

[a] Fructose/glucose mixture as substrate.

in a H_2O/MIBK biphasic system at catalytically relevant concentrations (0.1 g L^{-1} of H_2O), heated up to 150 °C and then cooled down to room temperature. This analysis included phthalic, isophthalic, terephthalic and *o*-toluic acid considering their simplicity, low cost and availability in our laboratory. In addition, EDTA was included in this analysis considering the previous reporting of this organic acid performing well in the conversion of sugars to HMF [29]. Fig. S5 shows the mass recovery of the acids after up to five cycles of the recoverability experiment. It can easily be seen that phthalic, isophthalic, terephthalic and *o*-toluic acid show poor ability to be recovered, highlighting *o*-toluic acid, whose loss is complete after only four cycles. In addition to the mass loss, the precipitation of these acids showed a flake-like shape rather than returning to a crystalline morphology, as observed in Figs. S6a and S6b for the cases of phthalic and isophthalic. The loss of mass of acid would obviously lead to a catalytic activity decline if used through different cycles and the flake-like morphology of the precipitate would complicate the recycling of the material. On the other hand, EDTA shows a very good behaviour with a loss of only as little as 5 % after five cycles of solution-precipitation and the material recovered showed the same morphology as freshly used, as seen in Fig. S6c. Fig. S7 shows the FTIR spectra of fresh EDTA as well as after some cycles of solution-precipitation, with virtually no changes. In addition, a TGA analysis of EDTA was conducted to check its stability through reaction cycles at relevant temperatures in this work (140–170 °C). As observed in Fig. S8, EDTA only starts decomposing from approximately 236 °C, significantly above the operating window, thus ensuring its thermal stability.

Considering this test, this acid was chosen to study its recyclability in reaction. For this, the catalytic performance of EDTA in reactions *a* and *b* was assessed in terms of substrate conversion, yield to product and turnover frequency (TOF). To ensure meaningful comparison of these metrics, it was decided to perform the recycling test at conditions below 50 % yield of the product, i.e., 423 K and 90 min for the case of HMF production and 433 K and 240 min for furfural production. Fig. 8 shows reaction performance after 5 cycles, where the catalyst was simply washed and dried between cycles. During these cycles, in reaction *a* the yield to the product HMF dropped from an initial 38.2 to 31.9 %, with a concomitant decline in TOF from 8.47 to 7.24, approximately 14.5 %. After these 5 cycles, it was decided to regenerate the catalyst by dissolving EDTA to separate it from possible humins formed, which were filtered out prior to reprecipitation of EDTA. Upon another cycle of use, the activity was recovered to 98 % of the TOF using fresh EDTA, as seen in Fig. 8a. The analysis in the case of reaction *b* is depicted in Fig. 8b, with similar numbers and conclusions. Here the decline in the TOF was about 13.2 % from the first to the fifth cycle and a recovery of 97 % of the initial activity after catalyst regeneration was observed, which suggests that the initially observed decline in catalytic activity was due to humin accumulation rather than the effect of subsequent solution-precipitation cycles to which EDTA is subjected.

3.4.2. Production of HMF and Fur using EDTA as catalyst

Similarly to the autocatalytic experiments, the progress of the reaction was analysed between 140 and 170 °C using a concentration of EDTA of 1 wt% based on the substrate load.

Fig. 9 shows the profile of the dehydration reaction of Fruc to HMF. As expected, the use of a catalyst accelerated the reaction, reaching almost full conversion of the substrate after 6 h at 150 °C compared toX_{Fruc} = 46.4 % in the autocatalytic case and full conversion in as short as 4 h and 2 h at 160 °C and 170 °C, respectively. Within the timeframe tested, maxima of concentrations of HMF were observed at the three highest temperatures, after which degradation to humins and rehydration to LA and FA become evident. At these points, selectivity values reached their peak, with values of S_{HMF} = 60.1 % after 4 h (at 150 °C), S_{HMF}=66.5 % after 2 h (at 160 °C) and S_{HMF} = 65.2 % after 90 min (at 170 °C). Comparing with the observations by Cao et al., our work shows X_{Fruc} = 90.3 % with the mentioned selectivity of 64.5 % at 160 °C after 2 h, whereas they reached values of X_{Fruc} = 98 % and S_{HMF} = 68 % under

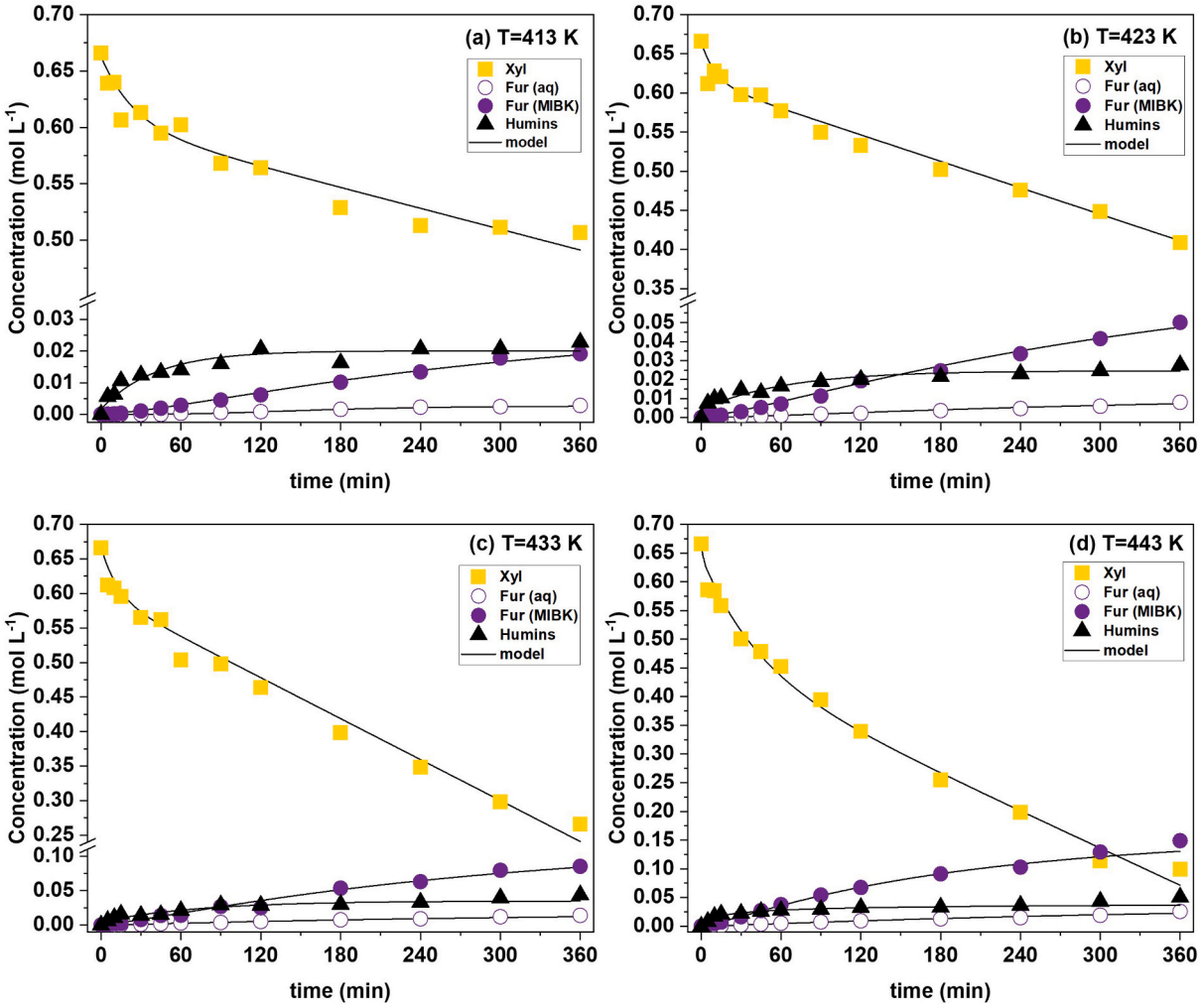

Fig. 11. Reaction profiles and model fittings for the production of Fur from Xyl (reaction *b*) with EDTA as catalyst in solution (*cs*) at (a) T = 140C; (b) T = 150C; (c) T = 160C; (d) T = 170C. Conditions: H_2O/MIBK = 1:3 v/v (V_{H2O} = 4 mL; V_{MIBK} = 12 mL); $C_{substrate}$ = 10 % wt·H_2O; substrate; ω = 400 rpm.

Table 5
Kinetic parameters and goodness of fit obtained from the fitting of the model for the dehydration of Xyl to Fur (reaction *b*) with EDTA as catalyst in solution (*cs*). Error in the parameters is given at 95% confidence interval.

Reaction	ln $k_{i,o}$ ± error	$E^{cs}_{a,i}/R$ ± error (K)	RMSE	VE (%)
$r^{cs}_{1,b}$	32.16 ± 4.46	15675 ± 1142	0.0804	98.01
$r^{cs}_{2,b}$	35.01 ± 3.88	11203 ± 897		
$r^{cs}_{3,b}$	29.52 ± 3.14	9633 ± 799		

similar operating conditions with a lower amount of catalyst employed, although using a different reaction setup [29]. This difference could be ascribed to our use of a microwave device compared to their conventional heating. EDTA has structural features that render microwave responsiveness that could accelerate catalytic activity, such as its multiple polar functional groups (four carboxylic functions) its ionic character in deprotonated form. Microwave irradiation has been used in EDTA-induced separations accelerating these processes [51,52]. Compared to the autocatalytic case, here it becomes more crucial to select an adequate reaction time to maximise the productivity towards the desired product and thus facilitate subsequent downstream separations.

Fig. 9 additionally shows the model fittings, in good agreement with the experimental observations, which is further depicted in the parity plot shown in Fig. 10a, where again most data fall within a ±10 % error with no general trend for over or underestimation of the data. This is confirmed by the low value of RMSE and high VE (96.41 %) obtained from the correlation, as summarised in Table 3 together with the fitted parameters. The values of activation energies of $E^{cs}_{a,1,a} = 139.12 \pm 8.40$ kJ mol^{-1}, $E^{cs}_{a,2,a} = 102.57 \pm 8.02$ kJ mol^{-1}, $E^{cs}_{a,3,a} = 134.82 \pm 10.15$ kJ mol^{-1}, $E^{cs}_{a,4,a} = 96.95 \pm 7.35$ kJ mol^{-1} and $E^{cs}_{a,5,a} = 97.55 \pm 8.74$ kJ mol^{-1}. These values are lower than those obtained for the autocatalytic ($E^{ac}_{a,i,a}$) reaction, which indicates the presence of this catalyst reduces the activation energy, as expected. Other studies have reported activation energies for the reactions associated with the production of HMF starting from Fruc as substrate (reactions $r^{cs}_{1,a}$ to $r^{cs}_{5,a}$ described in Fig. 3). Table 4 shows these values obtained, which were obtained in similar temperature range and either in monophasic or biphasic solvent systems. Here it is worthwhile discussing that, although most of the values we obtained for each of the reactions are similar, there are some differences. Two of them correspond to studies where only the activation energies for the main reaction of the network, the dehydration of fructose to HMF, where calculated, with values as low as 55 kJ mol^{-1} and a more similar value of 109 kJ mol^{-1} being reached [53]. In the former study, it is worth remarking that the authors only calculated the mentioned reaction, with no mention of formic or levulinic acids forming or contemplation of any other reaction in the network or extraction of any of the compounds since this was a monophasic system [54]. In the case of reaction *2a*, i.e., the rehydration to levulinic and formic acids, our results are similar to most other works that reported

Table 6
Comparison of the activation energies of the reactions involved in the production of the dehydration of Xyl to Fur (reaction *b*) catalysed with EDTA in solution (*cs*) obtained in this work with others reported in literature.

Reaction	Solvent system (aq:org v/v)	Catalyst	E_a(kJ mol^{-1})	T (K)	Ref.
$r^{cs}_{1,b}$	H_2O (monophasic)	H_2SO_4 0.1 M	166.2[a]	453–493	[59]
	Formic acid solution (monophasic)	$FeCl_3$ 0.2–0.8 M	67.2	373–443	[36]
	H_2O (monophasic)	NH_4Cl 500 mM	118.3 ± 0.4	413–473	[60]
	H_2O/1,4-dioxane (1:10)	[Bmim] HSO_4 IL:substrate ratio: 2:1–18:1	21.7	393–413	[61]
	H_2O/GVL (1:4)	HCl 10 mM	74.7 ± 2.9	473–513	[62]
	H_2O (monophasic)	H-BEA	30 ± 3	403–463	[30]
	H_2O/MIBK (1:3)	EDTA	130.33 ± 9.49	413–453	This work
$r^{cs}_{2,b}$	H_2O (monophasic)	H_2SO_4 0.1 M	162.9[a]	453–493	[59]
	Formic acid solution (monophasic)	$FeCl_3$ 0.2–0.8 M	99.5	373–443	[36]
	H_2O/1,4-dioxane (1:10)	[Bmim] HSO_4 2:1–18:1 IL: substrate ratio	7.1	393–413	[61]
	H_2O/GVL (1:4)	HCl 10 mM	118.6 ± 11.8	473–513	[62]
	H_2O (monophasic)	H-BEA	41 ± 7		[30]
	Water:MIBK (1:3)	EDTA	93.14 ± 7.46	413–453	This work
$r^{cs}_{3,b}$	H_2O (monophasic)	H_2SO_4 0.1 M	72[a]	453–493	[59]
	H_2O/1,4-dioxane (1:10)	[Bmim] HSO_4 IL:substrate ratio: 2:1–18:1	78.1	393–413	[61]
	H_2O/GVL (1:4)	HCl 10 mM	76.0 ± 8.4	473–513	[62]
	H_2O (monophasic)	H-BEA	31 ± 5	403–463	[30]
	H_2O/MIBK (1:3)	EDTA	80.08 ± 6.64	413–453	This work

[a] -modified Arrhenius equation $k_n = Ae^{\left(\frac{-E_{an}}{R}\left(\frac{T-T_{ref})}{TT_{ref}}\right)\right)}$ where T_{ref} = 408 K and a2 where T_{ref} = 413 K.

this reaction, with the exception of the case where the reaction was performed in a monophasic medium in the presence of LiCl [55]. In this case, the reaction network was modelled in a simpler manner, only obtaining humins separately from Fruc and HMF, although dismissing the joint generation of humins and FA starting from Fruc (reaction *3a*), which will have an effect on the fittings. It is remarkable that in this work no FA is accounted for in the models or reported at all, which makes it impossible for the consideration of reaction *3a*. Last, for the three reactions considering the generation of humins (reactions *3a*, *4a* and *5a*), our obtained activation energies are well aligned in general with the work by Guo et al. [11]. There are discrepancies in excess with respect to the values obtained in the aforementioned work owing to the more limited reaction model presented [55] and the monophasic reaction with HCl presented by Vlachos et al. [56,57], where the production of humins is modelled through the consideration of a lumped term from fructo-furanose, fructo-pyranose and open chain fructose as the three forms of Fruc.

Finally, the evolution of the species involved in reaction *b* in the presence of EDTA is shown in Fig. 11. As in reaction *a*, the catalyst has an obvious effect on the progress of the reaction, in which the conversion of the substrate and the yield to the product increase with respect to the autocatalytic case at comparable times and temperatures. Here, considering the lack of LA and FA in the reaction, only EDTA acts as additional source of acidity, hence making its presence key to the faster reaction rates observed. In this case, after 6 h at 140 °C, the conversion of the substrate is X_{Xyl} = 24 %, almost twice as high as the autocatalytic case, with a yield to the desired product of Y_{Fur} = 12.9 %, hence indicating a poor selectivity slightly over 50 % in that case; on the other hand, whereas after the same amount of time at 170 °C, the conversion achieved was X_{Xyl} = 87.1 %, with an overall furfural yield considering both phases of Y_{Fur} = 66.1 %, reaching a remarkable selectivity of S_{Fur} = 75.8 %, which confirms the usefulness of biphasic systems to enhance the effectiveness of the procedure. This is comparable to the high selectivity of 70 % observed in a previous work with the same H_2O/MIBK solvent system at a similar temperature of 175 °C [58].

Table 5 shows the values of the fitting parameters for reaction *b* in the presence of EDTA and the goodness of fit, which is also depicted in Fig. 10b through the parity plot of the predicted vs observed values. The model explains 97 % of the variation with a RMSE below 0.1. In this case, the activation energies observed were $E^{cs}_{a,1,b}$ = 130.33 ± 9.49 kJ mol^{-1} for the dehydration of Xyl to furfural ($r^{cs}_{1,b}$), $E^{cs}_{a,2,b}$ = 93.14 ± 7.46 kJ mol^{-1} for the degradation of Xyl to humins ($r^{cs}_{2,b}$) and, finally, $E^{cs}_{a,3,b}$ = 80.08 ± 6.64 kJ mol^{-1} for the generation of humins from furfural ($r^{cs}_{3,b}$). Again, these values are lower than the ones for the autocatalytic operation. Comparatively with other values reported in literature, as summarised in Table 6, our estimated activation energies are in the same order as other references, although there are some large differences with respect to others. For example, the activation energies obtained for reaction $r^{cs}_{1,b}$ is similar to those reported by Ershova et al. and Ricciardi et al. (166.2 and 118.3 kJ mol^{-1}, respectively) [59,60], but somewhat different to the values presented in other works. The use of H-BEA zeolite by Likozar et al. showed an activation energy of 30 kJ mol^{-1}, with this work showing a different reaction pathway than others with xylulose reacting to furfural through an unidentified intermediate, presumably xylulose or lyxose generated by the Lewis acidity of the catalyst. This intermediate then reacted to furfural with an activation energy of 99 kJ mol^{-1}, which is a more similar value to ours [30]. This same work also reports comparably low activation energies for reactions $r^{cs}_{2,b}$ and $r^{cs}_{3,b}$, only at 30 and 31 kJ mol^{-1}, respectively. This presumably responds to the fitting effects given the additional reactions considered in the network, particularly considering that the generation of humins through the intermediate has a value of 105 kJ mol^{-1}, more in line with our work and others. There are surprisingly low activitation energies in some cases both for furfural generation ($r^{cs}_{2,b}$), and humin formation hinting at an unusual activity for every reaction of the network with the ionic liquid [Bmim]HSO_4 as catalyst [61]. Less notable differences with other reported values also occur for reaction $r^{cs}_{2,b}$, whereas in the case of reaction $r^{cs}_{3,b}$ our results are in line with the references found. In addition to the fact that different catalysts are used in each case, another reason for the differences observed are the modified reaction pathways considered by each author, which has an obvious repercussion on the mass balances. For instance, some of the works report the presence of an intermediate species in the reaction, with furfural being generated through such intermediate in addition to the direct reaction from Xyl as starting chemical [30,59].

4. Conclusions

HMF and furfural can be obtained by the dehydration of fructose and

xylose, respectively, in a H_2O/MIBK biphasic system reaching notable selectivities to the products (up to approximately 70 % in the production of HMF and 75 % in the case of furfural). The operation can proceed both without catalyst and in the presence of a Brønsted acid. The former case represents the simplest biphasic operation that could be performed and for the latter, EDTA was identified as a thermoresponsive catalyst with remarkable recyclability returning to a catalytic activity greater than 97 % of the TOF observed with respect to fresh catalyst use after 5 cycles of use and facile regeneration.

Two models were developed for the reactions to produce HMF and furfural, applicable to the autocatalytic and EDTA-catalysed cases. These were described by the mass balances of the two reaction pathways and the biphasic operation assuming elementary reactions and power-law rate equations. Among the other main considerations featured in the model are: (a) the acidity of the medium being provided by the acidic species present, (b) an adjustment of the concentration values by the temperature effect on the change of the volume of each phase and (c) the assumption that the extraction of the soluble reaction products occurs instantaneously, with their concentrations in the extraction phase being proportional to the partition coefficient. With the use of microwave assisted operation, meaningful simplifications of the model could be made, highlighting the immediate dissolution of EDTA in the reaction medium and the negligible time needed to reach the set temperature of the reaction. For the dehydration of fructose to HMF, the autocatalytic reaction returned an activation energy of 155.72 ± 12.84 kJ mol^{-1}, whilst in the case of the EDTA-catalyzed reaction, the value was 139.12 ± 8.40 kJ mol^{-1}. For the dehydration of xylose to furfural, the fitted values for the activation energies are 138.09 ± 7.45 kJ mol^{-1} and 130.33 ± 9.49 kJ mol^{-1} for the autocatalytic and the EDTA-catalysed reaction. In all cases, the degree of fitting was very high, with variations explained above 96 % and RMSE below 0.13. This information is of relevance to further reactor design, subsequent process simulation and techno-economic analysis to test the viability of a process based on this concept.

Despite the water-based biphasic approach mitigating the generation of reaction by-products, further exploration on reaction kinetics remains an outstanding task for reactions using alternative media, such as deep eutectic solvents, which have proven to provide high furan yields [26,40].

CRediT authorship contribution statement

Nico Thanheuser: Writing – original draft, Visualization, Validation, Methodology, Investigation, Formal analysis, Data curation, Conceptualization. **Sebastian Püschel:** Visualization, Methodology, Investigation, Formal analysis. **Andreas J. Vorholt:** Writing – review & editing, Supervision, Resources, Project administration, Methodology, Investigation, Funding acquisition, Conceptualization. **Jesús Esteban:** Writing – review & editing, Writing – original draft, Supervision, Software, Methodology, Investigation, Funding acquisition, Formal analysis, Conceptualization.

Declaration of competing interest

The authors declare that they have no known competing financial interests or personal relationships that could have appeared to influence the work reported in this paper.

Acknowledgements

JE gratefully acknowledges grant RYC2022-035654-I funded by MICIU/AEI/10.13039/501100011033 and by ESF+ and grant PID2024-156902OA-I00 funded by MICIU/AEI/10.13039/501100011033 and ERDF/EU. The University of Manchester, the Max Planck Society and the Hermann Neuhaus Foundation for the Hermann Neuhaus Prize of 2020.

The RESCUE group at the University of Manchester is gratefully acknowledged for additional experimental work.

Appendix A. Supplementary material

Supplementary data to this article can be found online at https://doi.org/10.1016/j.fuel.2025.137934.

Data availability

Data will be made available on request.

References

[1] Bozell JJ, Petersen GR. Technology development for the production of biobased products from biorefinery carbohydrates—the US Department of Energy's "top 10" revisited. Green Chem 2010;12(4):539–54.
[2] Sajid M, Zhao X, Liu D. Production of 2,5-furandicarboxylic acid (FDCA) from 5-hydroxymethylfurfural (HMF): recent progress focusing on the chemical-catalytic routes. Green Chem 2018;20(24):5427–53.
[3] Przydacz M, Jędrzejczyk M, Rogowski J, Ihiawakrim D, Keller N, Ruppert AM. TiO2 supported non-noble Ni-Fe catalysts for the high yield production of 2,5-dimethylfuran biofuel. Fuel 2024;356:129606.
[4] Qiu Y, Liu H, Shan R, Zhao W, Zhang J, Zhang J, et al. Zr-decorated hyper-cross-linked polymers for highly selective upgrading of furfural to furfuryl alcohol. Fuel 2024;372:132291.
[5] Baldenhofer R, Smet A, Lange JP, Kersten SRA, Ruiz MP. Furanic jet fuels – water-free aldol condensation of furfural and cyclopentanone. Biomass Bioenergy 2024;190:107410.
[6] Esteban J, Vorholt AJ, Leitner W. An overview of the biphasic dehydration of sugars to 5-hydroxymethylfurfural and furfural: a rational selection of solvents using COSMO-RS and selection guides. Green Chem 2020;22(7):2097–128.
[7] Soukup-Carne D, Fan X, Esteban J. An overview and analysis of the thermodynamic and kinetic models used in the production of 5-hydroxymethylfurfural and furfural. Chem Eng J 2022;442:136313.
[8] Romo JE, Bollar NV, Zimmermann CJ, Wettstein SG. Conversion of sugars and biomass to furans using heterogeneous catalysts in biphasic solvent systems. ChemCatChem 2018;10(21):4805–16.
[9] Stankiewicz AI, Moulijn JA. Process intensification: transforming chemical engineering. Chem Eng Prog 2000;96(1):22–34.
[10] Aigner M, Roth D, Rußkamp J, Klankermayer J, Jupke A. Model-based equipment design for the biphasic production of 5-hydroxymethylfurfural in a tubular reactor. AIChE J;66(4):e16849.
[11] Guo W, Zhang Z, Hacking J, Heeres HJ, Yue J. Selective fructose dehydration to 5-hydroxymethylfurfural from a fructose-glucose mixture over a sulfuric acid catalyst in a biphasic system: experimental study and kinetic modelling. Chem Eng J 2021;409:128182.
[12] He X, Shi J, Gao C, Che W, Zeng X, Zuo M. Influence of oxygen-containing functional groups in sulfonated biochar on 5-hydroxymethylfurfural synthesis in aqueous solvents: mechanistic insights and theoretical analysis. Fuel 2025;395:135208.
[13] Labauze H, Camy S, Floquet P, Benjelloun-Mlayah B, Condoret J-S. Kinetic study of 5-hydroxymethylfurfural synthesis from fructose in high pressure CO2–water two-phase system. Ind Eng Chem Res 2019;58(1):92–100.
[14] Kumar M, Bains R, Chauhan AS, Kumar A, Das P. A straightforward process for conversion of de-oiled lemon grass (Cymbopogon citratus) waste into 5-hydroxymethylfurfural and furfural. Renew Energy 2025;244:122657.
[15] Long S, Li Y, Du F, Xian X, Tang P, Huang Z. Carbon materials as microwave absorbers for microwave-assisted conversion of sugars to 5-hydroxymethylfurfural in dimethyl carbonate-water solvents. Renew Energy 2025. 122921.
[16] Weingarten R, Cho J, Conner JWC, Huber GW. Kinetics of furfural production by dehydration of xylose in a biphasic reactor with microwave heating. Green Chem 2010;12(8):1423–9.
[17] Morais ARC, Bogel-Lukasik R. Highly efficient and selective CO2-adjunctive dehydration of xylose to furfural in aqueous media with THF. Green Chem 2016;18(8):2331–4.
[18] Román-Leshkov Y, Chheda JN, Dumesic JA. Phase modifiers promote efficient production of hydroxymethylfurfural from fructose. Science 2006;312(5782):1933–7.
[19] vom Stein T, Grande PM, Leitner W, de María PD. Iron-catalyzed furfural production in biobased biphasic systems: from pure sugars to direct use of crude xylose effluents as feedstock. ChemSusChem 2011;4(11):1592–4.
[20] Eifert T, Liauw MA. Process analytical technology (PAT) applied to biomass valorisation: a kinetic study on the multiphase dehydration of xylose to furfural. React Chem Eng 2016;1(5):521–32.
[21] Sato O, Mimura N, Masuda Y, Shirai M, Yamaguchi A. Effect of extraction on furfural production by solid acid-catalyzed xylose dehydration in water. J Supercrit Fluids 2019;144:14–8.
[22] Tongtummachat T, Akkarawatkhoosith N, Jaree A. Process intensification for 5-hydroxymethylfurfural production from sucrose in a continuous fixed-bed reactor. Chem Eng Res Des 2022;182:312–23.
[23] Xiang H, Zainal S, Jones H, Ou X, D'Agostino C, Esteban J, et al. Hierarchical zeolite catalysed fructose dehydration to 5-hydroxymethylfurfural within a

biphasic solvent system under microwave irradiation. RSC Sustain 2023;1(6):1530–9.
[24] Xu S, Pan D, Hu F, Wu Y, Wang H, Chen Y, et al. Highly efficient Cr/β zeolite catalyst for conversion of carbohydrates into 5-hydroxymethylfurfural: characterization and performance. Fuel Process Technol 2019;190:38–46.
[25] Koley P, Shit SC, Yoshida T, Ariga-Miwa H, Uruga T, Hosseinnejad T, et al. Elucidation of active sites and mechanistic pathways of a heteropolyacid/Cu-metal-organic framework catalyst for selective oxidation of 5-hydroxymethylfurfural via Ex situ X-ray absorption spectroscopy and in situ attenuated total reflection-infrared studies. ACS Catal 2023;13(9):6076–92.
[26] Thanheuser N, Groteguth JT, Leitner W, Esteban J, Vorholt AJ. Biphasic Production of 5-hydroxymethylfurfural (HMF) in a Recyclable Deep Eutectic Solvent-based System Catalyzed by H4SiW12O40. ChemSusChem 2025;18(3):e202401485.
[27] Chen S, Lin X, Zhai Z, Lan R, Li J, Wang Y, et al. Synthesis and characterization of CO2-sensitive temperature-responsive catalytic poly(ionic liquid) microgels. Polym Chem 2018;9(21):2887–96.
[28] Lou L-L, Qu H, Yu W, Wang B, Ouyang L, Liu S, et al. Covalently immobilized lipase on a thermoresponsive polymer with an upper critical solution temperature as an efficient and recyclable asymmetric catalyst in aqueous media. ChemCatChem 2018;10(5):1166–72.
[29] Cao Z, Li M, Chen Y, Shen T, Tang CL, Zhu CJ, et al. Dehydration of fructose into 5-hydroxymethylfurfural in a biphasic system using EDTA as a temperature-responsive catalyst. Appl Catal A 2019;569:93–100.
[30] Jakob A, Likozar B, Grilc M. Aqueous conversion of monosaccharides to furans: were we wrong all along to use catalysts? Green Chem 2022;24(21):8523–37.
[31] Jing Q, Lü X. Kinetics of non-catalyzed decomposition of D-xylose in high temperature liquid water. Chin J Chem Eng 2007;15(5):666–9.
[32] Fachri BA, Abdilla RM, Bovenkamp HHvd, Rasrendra CB, Heeres HJ. Experimental and Kinetic Modeling Studies on the Sulfuric Acid Catalyzed Conversion of d-Fructose to 5-Hydroxymethylfurfural and Levulinic Acid in Water. ACS Sustain Chem Eng 2015;3(12):3024-34.
[33] Gan L, Lyu L, Shen T, Wang S. Sulfonated lignin-derived ordered mesoporous carbon with highly selective and recyclable catalysis for the conversion of fructose into 5-hydroxymethylfurfural. Appl Catal A 2019;574:132–43.
[34] Girisuta B, Janssen LPBM, Heeres HJ. A kinetic study on the decomposition of 5-hydroxymethylfurfural into levulinic acid. Green Chem 2006;8(8):701–9.
[35] Lamminpää K, Ahola J, Tanskanen J. Kinetics of xylose dehydration into furfural in formic acid. Ind Eng Chem Res 2012;51(18):6297–303.
[36] Lopes M, Dussan K, Leahy JJ. Enhancing the conversion of D-xylose into furfural at low temperatures using chloride salts as co-catalysts: catalytic combination of AlCl3 and formic acid. Chem Eng J 2017;323:278–86.
[37] Weiqi W, Shubin W. Experimental and kinetic study of glucose conversion to levulinic acid catalyzed by synergy of Lewis and Brønsted acids. Chem Eng J 2017;307:389–98.
[38] Wang F, Zhao H, Zhang Y, Song F, Tan H, Yu F, et al. Kinetic and characteristic investigations on the conversion of cellulose to 5-hydroxymethylfurfural in the mixed metal salt system. Renew Energy 2025;242:122434.
[39] Prat D, Wells A, Hayler J, Sneddon H, McElroy CR, Abou-Shehada S, et al. CHEM21 selection guide of classical- and less classical-solvents. Green Chem 2016;18(1):288–96.
[40] Thanheuser N, Schlichter L, Leitner W, Esteban J, Vorholt AJ. 5-Hydroxymethylfurfural (HMF) synthesis in a deep eutectic solvent-based biphasic system: closing the loop of solvent reuse, product isolation and green metrics. RSC Sustain 2025;3:1848–58.
[41] Esteban J, Fuente E, Blanco A, Ladero M, Garcia-Ochoa F. Phenomenological kinetic model of the synthesis of glycerol carbonate assisted by focused beam reflectance measurements. Chem Eng J 2015;260:434–43.
[42] Soukup-Carne D, Hillman B, Parlett CMA, Fan X, Esteban J. Dehydration of xylose to furfural in a biphasic system: catalyst selection and kinetic modelling discrimination. React Chem Eng 2025.
[43] Yang T, Zhou Y-H, Zhu S-Z, Pan H, Huang Y-B. Insight into aluminum sulfate-catalyzed xylan conversion into furfural in a γ-valerolactone/water biphasic solvent under microwave conditions. ChemSusChem 2017;10(20):4066–79.
[44] Ma H, Wang F, Yu Y, Wang L, Li X. Autocatalytic production of 5-hydroxymethylfurfural from fructose-based carbohydrates in a biphasic system and its purification. Ind Eng Chem Res 2015;54(10):2657–66.
[45] Tang J, Zhu L, Fu X, Dai J, Guo X, Hu C. Insights into the kinetics and reaction network of aluminum chloride-catalyzed conversion of glucose in NaCl–H2O/THF biphasic system. ACS Catal 2017;7(1):256–66.
[46] Bianga J, Künnemann KU, Gaide T, Vorholt AJ, Seidensticker T, Dreimann JM, et al. Thermomorphic multiphase systems: switchable solvent mixtures for the recovery of homogeneous catalysts in batch and flow processes. Chem Eur J 2019;25(50):11586–608.
[47] Han N, Zhu L, Wang L, Fu R. Aqueous solubility of m-phthalic acid, o-phthalic acid and p-phthalic acid from 298 to 483 K. Sep Purif Technol 1999;16(2):175–80.
[48] Ren B-Z, Hou C-H, Chong H-G, Li W-R, Song H-J. Solubility of o-phthalic acid in methanol + water and methanol + butyl acetate from (295.87 to 359.75) K. J Chem Eng Data 2006;51(6):2022–5.
[49] Shen Z, Wang Q, Chen L, Sheng X, Pei Y. Solubilities of phthalic acid and o-toluic acid in binary acetic acid + water and acetic acid + o-xylene solvent mixtures. J Chem Eng Data 2016;61(9):3233–40.
[50] Sunsandee N, Hronec M, Štolcová M, Leepipatpiboon N, Pancharoen U. Thermodynamics of the solubility of 4-acetylbenzoic acid in different solvents from 303.15 to 473.15K. J Mol Liq 2013;180:252–9.
[51] Barnett C, Huerta-Munoz U, James R, Pauls G. The use of microwave radiation in combination with EDTA as an outer membrane disruption technique to preserve metalloenzyme activity in *Escherichia coli*. J Exp Microbiol Immunol 2006;9:1–5.
[52] Öztan S, Düring R-A. Microwave assisted EDTA extraction—determination of pseudo total contents of distinct trace elements in solid environmental matrices. Talanta 2012;99:594–602.
[53] Mellmer MA, Sanpitakseree C, Demir B, Ma K, Elliott WA, Bai P, et al. Effects of chloride ions in acid-catalyzed biomass dehydration reactions in polar aprotic solvents. Nat Commun 2019;10(1):1132.
[54] Chen J, Li K, Chen L, Liu R, Huang X, Ye D. Conversion of fructose into 5-hydroxymethylfurfural catalyzed by recyclable sulfonic acid-functionalized metal–organic frameworks. Green Chem 2014;16(5):2490–9.
[55] Wang J, Cui H, Wang J, Li Z, Wang M, Yi W. Kinetic insight into glucose conversion to 5-hydroxymethyl furfural and levulinic acid in LiCl·3H2O without additional catalyst. Chem Eng J 2021;415:128922.
[56] Swift TD, Bagia C, Choudhary V, Peklaris G, Nikolakis V, Vlachos DG. Correction to kinetics of homogeneous brønsted acid catalyzed fructose dehydration and 5-hydroxymethyl furfural rehydration: a combined experimental and computational study. ACS Catal 2014;4(5). 1320-.
[57] Swift TD, Bagia C, Choudhary V, Peklaris G, Nikolakis V, Vlachos DG. Kinetics of homogeneous brønsted acid catalyzed fructose dehydration and 5-hydroxymethyl furfural rehydration: a combined experimental and computational study. ACS Catal 2014;4(1):259–67.
[58] Antonyraj CA, Haridas A. A lignin-derived sulphated carbon for acid catalyzed transformations of bio-derived sugars. Catal Commun 2018;104:101–5.
[59] Ershova O, Kanervo J, Hellsten S, Sixta H. The role of xylulose as an intermediate in xylose conversion to furfural: insights via experiments and kinetic modelling. RSC Adv 2015;5(82):66727–37.
[60] Ricciardi L, Verboom W, Lange J-P, Huskens J. Local overheating explains the rate enhancement of xylose dehydration under microwave heating. ACS Sustain Chem Eng 2019;7(16). 14273-+.
[61] Xia Q, Peng H, Zhang Y, Fu G, Liu Y, Xiao Z, et al. Microwave-assisted furfural production from xylose and bamboo hemicellulose in a biphasic medium. Biomass Convers Biorefin 2023;13:7895–907.
[62] Sener C, Motagamwala AH, Alonso DM, Dumesic JA. Enhanced furfural yields from Xylose dehydration in the γ-valerolactone/water solvent system at elevated temperatures. ChemSusChem 2018;11(14):2321–31.